Blind Watermark Algorithm Based on HVS and RBF Neural Network in DWT Domain

YANHONG ZHANG
School of Computer Science and Information Technology
Zhejiang Wanli University
NingBo, Zhejiang 315100
P.R.CHINA
http://www.zwu.edu.cn

Abstract: - This paper proposes a new blind watermarking scheme based on discrete wavelet transform(DWT) domain. The method uses the HVS model, and radial basis function neural networks(RBF). RBF will be implemented while embedding and extracting watermark. The human visual system (HVS) model is used to determine the watermark insertion strength. The neural networks almost exactly recover the watermarking signals from the watermarked images after training and learning. The experimental results show that the watermark proposed in this paper is invisible (the PSNR is higher than 41) and is robust in the case of against some normal at tacks such as JPEG compression , additive noise and filtering , etc.

Key-Words: - blind digital watermarking, wavelet transform, RBF neural network, robustness

1 Introduction

The massive spreading of broadband networks and new developments in digital technology has made ownership protection and authentication of digital multimedia a very important issue. As a solution to this problem, digital watermark technology is now drawing the attention as a new method of protecting copyrights for digital data[1]. It is realized by embedding information data with an insensible form for human audio/visual systems. We call the embedded information data watermark.

At present, most of digital watermarking algorithm that combine spatial and transform domain use the human visual model of intensity and texture characteristics of shelter, that is, higher the brightness of the general background, and the more complex texture, the more insensitive of mankind vision for them slighter changes[2]. One of the most typical algorithm is put forward by PODICHU KCI, using visual model to determine the location that the watermark image is embedded in and the maximum strength of the watermark. A binary watermark sequence is embedded into the highest magnitude DCT coefficients. Hence, this algorithm is robust against image processing and common geometric transformations. Hsu and Wu proposed discrete cosine/wavelet transform algorithms to embed a binary watermark by modifying the middle-frequency coefficients. This algorithm is resistant to common image processing, but geometric distortions are still challenges. The main drawback is requiring the original image to detect/extract the watermark. Recently, a grayscale digital watermarking technique was proposed by Niu *et al.* The gray scale watermark, a visually recognizable pattern, is decomposed into eight binary bitplanes. Some binary bitplanes are embedded with the remainder used as the secret keys[3-5].

Today, almost all of the proposed watermark algorithms could not meet the above requirements, combined with spatial and transform domain algorithm has yet to be resolved include:

(1)Three basic requirements on digital watermarking: robustness, perceptual transparency and capacity. They are in conflict which each other. If the embedded watermark shall be robust against attacks we have to increase the energy of watermark but on the other hand we get the problem with perceptual transparency requirement. Vice versa if we want a very good perceptual transparency of embedded watermark we have to decrease the watermark energy but at the same time a problem of watermark robustness arises. The proper selection of signal components or coefficients for watermark embedding and the allowed amount of modification of these signal components in watermark embedding process is therefore a very important issue. A very effective solution of this problem can be achieved by using of human visual system(HVS) models. HVS models in transform domain of DCT and DWT were originally developed for image compression based on DCT and DWT where there has been a need of a good quantization matrix that would provide better quality of compressed images with higher compression ratio[6-7].

(2)Blind watermarking is not easy to achieve. At present, the algorithm based on the traditional visual transform domain model of the digital watermarking needs to compare watermark image with the original image to extract the watermark. As a matter of fact, the demand for the needs of blind watermark detection have a high proportion. The non-blind watermarking methods are very effective both in terms of image quality and robustness against various attacks. However the blind watermarking technique, which doesn't require the original image while detecting watermark, is widely used in watermarking area[8].

(3)Low security is another problem. As the algorithm using visual mask to choose the location of the watermark embedded has been widely used, so in accordance with this algorithm to extract the watermark complexity is not high, is not conducive to confidential communications[9-10].

In this paper, a new blind watermark embedding/extracting algorithm using the RBF neural networks is introduced. The DWT is used to overcome the blocking phenomenon problems in DCT. First, the original image is 4-scale level DWT transformed, and decided the watermarking strength according to HVS. When embedding watermark, a secret key is used to determine the watermark embedding beginning location, and after that, embed and extract the watermark by using the trained RBF. The experimental results show that the watermark proposed in this paper is invisible (the PSNR is higher than 41) and is robust in the case of against some normal image processing attacks.

2 Related Theories

2.1 Construction of HVS Model

Most HVS models in image processing use three basic properties of human vision: frequency sensitivity, luminance sensitivity and masking effects. Frequency sensitivity determines the human's eye sensitivity to various spatial frequencies. Luminance sensitivity measures the effect of the detectable threshold of noise on a constant background. It is the correction of frequency sensitivity according to the change of background luminance. Masking refers to the effect of decreasing visibility of one signal in the presence of another signal called masker. We can distinguish self masking and neighborhood masking. Self masking is when masking and masked signal have the same spatial frequencies, orientation and location in an image. Neighborhood masking refers to the masking where these signals have close spatial frequencies, orientation or location in an image.

2.2 Discrete Wavelet Transform (DWT)

Gabor in 1945 introduced the basic idea of wavelet theory. Considerable part has been made further improve on Discrete Wavelet transformation(DWT). The greatest contribution in DWT development has come from signal and image processing.

DWT has the ability to express the local characteristics of the signal both spatial and temporal domains. These wavelets enable us to decompose an image in both spatial and temporal domains. It not only can better match the human visual system characteristics, and also JPEG2000 standard, the embedded watermark in DWT domain is of great significance. As we all know, using wavelet transform, an image can be decomposed into the low frequency component and three high-frequency components along different directions (horizontal, vertical and diagonal direction)[11-12]. The low-frequency component contains the average information and most of the energy of the image, while the high-frequency components contain the details of the images.

The fundamental idea behind wavelet is to analyze according to scale and time. It is well known that Fourier Transform can transform a signal from spatial domain to a frequency domain. One big disadvantage of Fourier Transform is that one can only represent a signal with frequency resolution without any time resolution or spatial information.In wavelet analysis, temporal analysis is performed with a contracted, high-frequency basis function, and frequency analysis is performed with a dilated, low-frequency basis function. Haar wavelet (Daubechies-1) is one of Daubechies wavelets members that is very popular because of its simple interpolation schema. Haar wavelet uses two types oflters. One is a low-pass filter and the other is a high-pass filter. The output of the low-pass filter is obtained by averaging the input,while the output of high-pass filter is obtained from the dierence of the inputs. One can easily conclude that the low-pass lter contains more information than high-pass filter because most of the signal energy is concentrated in low-pass filter. Daubechies-4 wavelet, on the other hand, splits the input signal by using four kinds of filters (LL, LH, HL, HH) with most of the energy concentrating in LL sub-band (L stands for low, while H stands for high).It has slightly computational overhead and is more complex than

Haar wavelet, but it is capable of including more details than Haar wavelet algorithm.

The wavelet transform is a mathematical tool for decomposing.We briefly review the DWT model(Fig.1),which shows a schematic diagram of wavelet transform. The image is first decomposed into four sub-bands denoting LL1,LH1,HL1 and HH1. LH1,HL1 and HH1 contain the finest scale detailed wavelet confficients,that is to say ,the higher frequency detailed information.LL1,the coarse overall shape,is the low frequency component containing most of the energy in the image.The wavlet transform is then applied to obtain the next coarser scale by further decomposing LL1 into LL2,LH2,HL2 and HH2,if the process is repeated t times,we can botain the sub-band LLt through t-scale level wavelet transform.

In the human visual system,people are more sensitive to low frequency components than high frequency components.The LL sub-band is realistic sub-band, contains important information not suitable for the embedded watermark, or gives rise to distortion of the image and perception by the human eye.

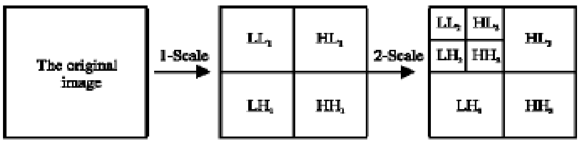

Fig.1. 2-scale level Wavelet transformation

2.3 HVS Model in DWT Domain

In most of the HVS-based DWT domain digital watermarking algorithm, the watermark is embedded in the wavelet sub-band frequency, here, in the watermarking algorithm proposed in this paper, the watermark is embedded in high-frequency part of the wavelet coefficients, so not only increases the intensity of the embedded watermark, At the same time maintain the invisibility of the embedded watermark[14-15].

Visibility thresholds of frequency sensitivity $T_{l,\Omega}$, in various sub-bands for 9/7 biorthogonal wavelets were determined via psychological experiments and can be expressed by the following equation 1.

$$T_{L,\Omega} = \frac{T_{\min}}{A_{L,\Omega}} 10^{S\left(\log\frac{r}{2^L f_0 g_\Omega}\right)^2} \qquad (1)$$

Where $A_{L,\Omega}$, are the basis function amplitudes, $T_{\min}$ is the minimum threshold occurs at spatial frequency $g_\Omega f_\Omega$, f_l is the spatial frequency of decomposition level L and g_Ω shifts the minimum thresholds by an amount that is a function of orientation.

Similarly as in the case of DCT domain, thresholds of frequency sensitivity are weighted by HVS model based on ROI according to the equation 2.

$$T^f(L,\Omega,m,n) = T_{L,\Omega}\cdot\left(1+\frac{\beta.T_{ROI}^{L,\Omega}(m,n)}{100.\max\left(T_{ROI}^{L,\Omega}\right)}\right) \qquad (2)$$

Where $T_{ROI}^{L,\Omega}(m,n)$ are T_{ROI} thresholds in sub-band L,Ω. An example of HVS model based on weighted frequency sensitivity thresholds is shown in Fig. 2.

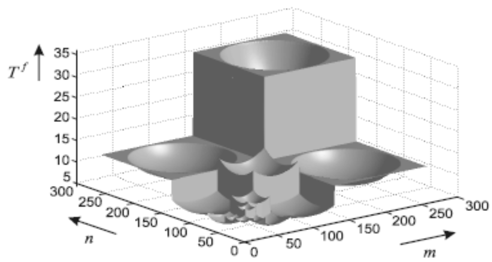

Fig. 2. weighted frequency sensitivity thresholds of HVS model in DWT domain.

In this paper, the linear-phase 9/7 biorthogonal filters are used for DWT, and the watermark is embedded into LL1, LH_1, HL_1, and HH_1 frequency band for robustness. We 494 C.-R. Piao et al. also use HVS to decide the watermarking strength of DWT coefficients. The HVS presented by Watson et al. for biorthogonal wavelet basis 9/7, gained the value of quantization matrix. From the quantization matrix, the maximal values of quantization error in LL1, LH_1, HL_1, and HH_1 band is about 7. So the random sequence value should be resisted in the range of $|wi|<7$ in this paper.

2.4 RBF (The Radial Basis Function Neural Networks)

Neural network is a potential tool in most of the signal processing and other application. Digital watermarking is not an exception where it finds a way to use neural network in order to make the process more secure and robust .Different models of neural network have their own merits and demerits. In this study, a RBF neural network and DWT based digital watermarking technique is proposed to gain in computational efficiency as well as memory requirements. The scheme is also more secure and robust.

The radial basis function (RBF) neural network has an universal approximation capability and has been successfully applied to many signal and image processing problems. A RBF network is a fully connected network and generally is used as a classification tool. In a RBF model, the layer from input nodes to hidden neurons is unsupervised and the layer from hidden neurons to output nodes is supervised. The transformation from the input to the hidden space is nonlinear, and the transformation from the hidden to the output space is linear. The hidden neurons provide a set of 'functions' that constitute an arbitrary 'basis' for the input patterns. These are the functions known as radial basis functions. Through careful design, it is possible to reduce a pattern in a high-dimensional space at input units to a low-dimensional space at hidden units. RBF neural network makes use of weighted sum of the Gaussian basic function with diagonal covariance matrix as posterior probability of training data[13].

In Figure 3, the network forms the following equation 3:

$$y_k(x) = w_{k0} + \sum w_{kj} h_j(x). \quad (3)$$

Where $h_j(x)$ is a Gaussian function typically, and w_{k0} is the bias or threshold. The Gaussian basis function is used as an activation function. That is following equation 4.

$$h_j(x) = \exp\left(-\sum \frac{(x - \mu_j)^2}{2\sigma_j^2}\right) \quad (4)$$

Fig.3 shows the basic structure of RBF, RBF has basic function layer and linear discrete layer.

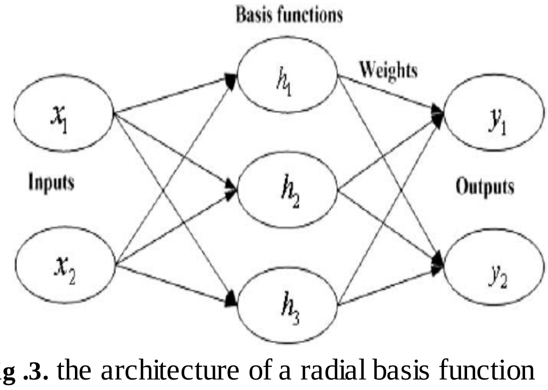

Fig .3. the architecture of a radial basis function neural network.

The input vector has d nodes and the outputs vector has c nodes. It is a mapping from $R^d \rightarrow R^c$.

Where X is the d-dimensional input vector with elements x_i, and μ_j and σ_j are, respectively, the center and the standard deviation of the Gaussian basis function. Since the first and second layers of RBF network are unsupervised and supervised, respectively, a two-stage training procedure is used for training the RBF model. In the first stage, the input data set is used to obtain the parameters of the activation functions (like μ_j and σ_j). In the second stage, the optimal weights between hidden neurons and output nodes are obtained by minimizing a sum-of-square error function. The following procedures describe the steps of obtaining the optimal weights. By absorbing the bias parameter, w_{k0}, into the weights, Equation 5 can be revised as

$$y_k(\mathrm{X}) = \sum w_{kj} h_j(\mathrm{X}) \quad (5)$$

Where $h_j(X)$ is an extra basis function with the activation value 1. Equation 6 can be rewritten using matrix notation as

$$Y(X) = W\Phi \quad (6)$$

Where $W = [w_{kj}]$ and $\Phi = [h_j(X)]$.The sum-of-square error function, E, can be described as equation 7.

$$E = \frac{1}{2} \sum \sum (y_k(X^n) - t_k^n)^2 \quad (7)$$

Where X^n is the input data set, and t_k^n is the target value for the output unit k. By differentiating E with respect to w_{kj} and setting derivative to zero, the optimal weights can be obtained. The solutions of weights can be expressed using matrix notation as equation 8.

$$(\Phi^T \Phi) W^T = \Phi^T T \quad (8)$$

Where $T = [t_k^n]$ and $\Phi = [h_j(X^n)]$

By multiplying $(\Phi^T \Phi)^{-1}$ to Equation (8), the solution for the weights is given as equation 9 and equation 10.

$$W^T = (\Phi^T \Phi)^{-1} \Phi^T T \quad (9)$$

$$W^T = \Phi^+ T \quad (10)$$

Where $\Phi^+ = (\Phi^T \Phi)^{-1}$ is the pseudo-inverse of Φ.After computing the optimal weights, the RBF network can be used as a classifier to segment the test data into the corresponding classes, with-1 indicating a non-flare state and 1 indicating a flare state.

RBF is strongly dependent on the quality of the employed learning strategy and the quantity of training images. The aim of an adaptive learning RBF network is to reduce the required knowledge of the system parameters with a minimum amount of performance loss. The RBF network requires knowledge of three different parameters per neuron:

– The center vector μ_j.

– The weights W_{kj}.

– The radius σ_j.

One unsupervised learning strategy is the self-organizing feature map.

When the algorithm has converged, prototype vectors which correspond to nearby points on the feature map grid have nearby locations in input space. However, the imposition of the topographic property, particularly if the data is not intrinsically two-dimensional, may lead to a sub-optimal placement of vectors. Here we use the K-means unsupervised learning strategy as follows. Let μ_j be the mean of the data points in set S_j given by equation 11.

$$\mu_j = \frac{1}{N}\sum_{n \in S_J} X^n \qquad (11)$$

The initial centers are randomly chosen from the data points, and the nearest μ_j. is updated using equation 12.

$$\Delta\mu_j = \eta \left\| \mathrm{X}^n - \mu_j \right\| \qquad (12)$$

Where η is the learning rate parameter.

The second parameter of the RBF network is the weight w_k of the output layer.The weights can be summarized as equation 13.

$$\Delta W = 2\eta(y_k(\mathrm{X}^n) - t_k^n)h(\mathrm{X}^n) \quad (13)$$

Where η is the learning rate of LMS, and yk(xn) and tnk are the responses of the RBF network and the desired response, respectively. The vector h(xn) contains the unweighted responses of all neurons in the hidden layer.

The last parameter of the RBF network is the radius or spread of the radial function. We may use an average of the center spread of all RBFs to calculate the radius. After the centers μ_j are established, σ^2 can be derived from the center as equation 14.

$$\sigma^2 = \frac{1}{M}\sum_{j=1}^{M} \|\mathbf{x}^n - \mu_j\|^2, \qquad (14)$$

Where M is the number of hidden nodes.The feature information is in the center and the width of the basic function (μ_j, σ_j), the weight w_{kj} shows the important of basic function for input. In this article, the center of basis function is 0 , width is 1.

2.5 RBF simulation quantitative reverse procedure

The realization of mapping and function approximation is a common feature of the feed-forward network, RBF network (RBF network) with a strong input and output Mapping function, and was proved the Optimal network to Complete the mapping function in theory.

RBF nueral network has been a great success in many applications, especially in the respect of Pattern Classification and function approximation and classification, for its simple network structure, the rapid process of training , the good ability of promotion, and many other advantages. Therefore, in this paper, we use the RBF training to simulate the procedure of inverse image quantification to obtain the quantitative characteristics of original image, after the watermark embedded in, use neural networks to eliminate effectively the interference from quantification procedure for image, use the good traininged RBF network to extracte the Watermark, to ensure watermark robustness[16]. RBF neural network training process shown in Fig. 4.

2.6 The Radial Basis Function Neural Networks (RBF) and Training Procedures

In this paper, the data are used to approximate a linear function, and RBF neural network is implemented. Radial basis function networks have a basis function layer and a linear discriminating layer. RBF networks represent the posterior probabilities of the training data by a weighted sum of Gaussian basis functions with diagonal covariance matrices. The information is stored in the centers and the width of the basis functions and the center is set to zero while the width is set to one. RBF will be used to learn the characteristics of image for improving the performance of watermarking scheme. The RBF neural network training procedures are as Fig.4.

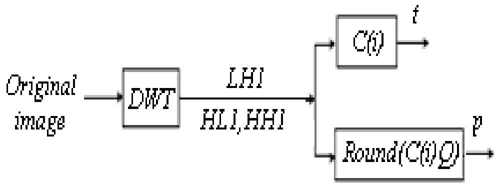

Fig.4. RBF simulation quantitative reverse the course of the training process.

In Fig.4, *C(i)* is the LH_i, HL_i and HH_i sub- band coefficient when DWT transform is performed on original image, *Q* is the quantization value, *p* is the output of quantization procedure, as an input value for the RBF, t is selected for the DC component of the original value, as the desired output value for RBF.

3. Watermark Embedding and Extracting

3.1 Selection of the wavelet decomposing scale t:

We know that, as the wavelet decomposed scale t increasing, the amplitude of low frequency coefficient increases with the approximate 2 multiple. Usually, the watermark is thought to be a weak signal added to strong background(the original image).So long as the weak signal added is lower than the contrast sensitivity threshold, the human vision system can't feel its existence. According to Weber's law, the contrast sensitivity threshold is proportional to amplitude of the background signal. This shows that, as the wavelet decomposed scale t increasing, strength of embedding watermark can increase with approximate 2 multiple.

As the wavelet decomposed scale t increasing, strength of embedding watermark will increase significantly. Thus, robustness of the watermark may be improved. Moreover, the more wavelet decomposed scale t, the better components of watermark can be spread. So, for the watermark algorithms, the wavelet decompose scales should be improved possibly according to the amount of the watermark data.

3.2 Watermark Embedding

In present experiments, the original image is 4-scale level wavelet transformed and the quantization step value are Q_1=16 and Q_2=6, respectively. For evaluate the quality the test image and the original image using the Peak Signal-to-noise Ration (PSNR). HL_4, LH_4 and HH_4, sub-band of image after 4-scale level wavelet transform to embed watermark..Fig.5 is a schematic diagram of the three-wavelet transform.LL_4 for the first layer of 4-scale level Low-frequency coefficients, which contains the main content of the image. HL_4, LH_4 and HH_4 corresponding layer of vertical, horizontal and diagonal high-frequency information, include the main part of the image details.

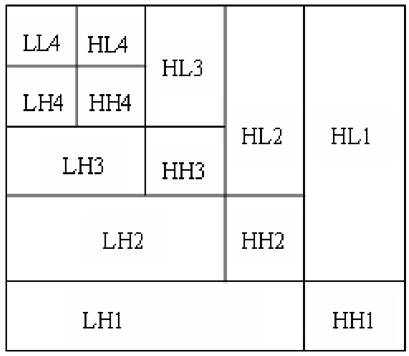

Fig.5. 4-scale level Wavelet transformation

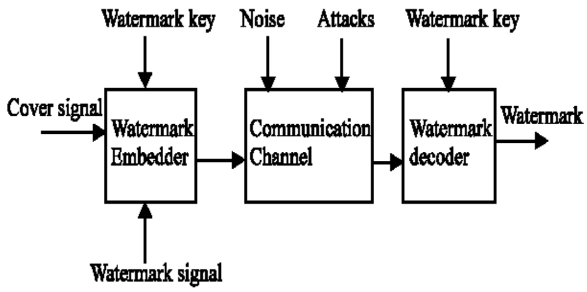

Fig. 6. digital watermarking system

Fig. 6 shows digital watermarking system and the embedding procedures are as follows:

Step1: Transform an original image using the DWT transform. In Fig. 4, *C(i)* is the LH_4, HL_4, HH_4 sub-band coefficient.

Step2: Select the beginning position of watermark embedding coefficient *C(i)* using the secret key.

Step3: Quantize the DWT coefficient $C_{(i+key)}$ by *Q*, as the input value of RBF then get the output $RBF(Round(C_{(i+key)}/Q))$

Step4: Embed the watermark according to the equation 15 which uses the output value of the RBF neural network (*RBF(round(C(i+key)/Q))*)and the *Q*.

$$C'_{i+key} = RBF(Round(C_{i+key}/Q)) + x_i(|x_i| \le 7) \quad (15)$$

Where x_i is the random sequence watermark, Q is a quantization value, and C'_{I+KEY} is the coefficient value when watermark is embedded. Then perform DWT to get the watermarked image[17].

3.3 Watermark Extracting

The watermark extracting procedures are as follows:

Step1: Transform the watermarked image by the DWT transform. In Fig.4,*C''(i)* is theLH_4, $HL_4$and HH_4 sub-band coefficient.

Step2: Quantize the DWT coefficient *C''(i)* by *Q*, as the input value of RBF then get the output *RBF(Round(C''(i)/Q))*.

Step3: Extract the watermark (x_i') using the equation 16 below, using the output of the RBF neural network (*RBF(Round(C''(i)/Q))*) and coefficient *C''(i)*.

$$x_i' = c''(i) - RBF(Round(c''(i)/Q)) \qquad (16)$$

Step 4: Measure the similarity(NC) of the extracted watermark *x'* and the original watermark *x* by equation 17.

$$sim(x, x') = x' \cdot x / \sqrt{x' \cdot x'} \qquad (17)$$

Step 5: Use *sim*(*x, x'*), threshold, as a key to judge if there is a embedded watermark or not. If *sim*(*x, x'*) is larger than threshold and the location is equal to the key, the watermark can be affirmed . The threshold is determined by standard deviation and false positive error probability that is implemented as 10-6. Based on those values, the threshold value is set to 20.8.

4 Experimental Results and Conclusions

The algorithm is simulated using MATLAB.Fig.7 shows the original image and watermarked image. Standard 256 gray scale image Lena of size 512×512 is chosen as the original image , 256 gray scale image 128 × 128 Barbara is used as watermark image. The image quality metric is based on the PSNR. The PSNR of the watermarked image is decreasing with increasing *Q*, but the PSNR is bigger than 41dB in any case. This paper proposes a new blind watermarking scheme in which a watermark is embedded into the DWT domain. It also utilizes RBF, which learns the characteristic of the image, and then watermark will be embedded and extracted using the trained RBF neural network.Fig.8 shows the classify results of wavelet transformation sub-band coefficient.

Fig. 7. (a) original image

(b)watermark (Barbara)

(c) watermarked image (PSNR=41.53 dB)

(d) retrieved watermark(BCR=93.86%)

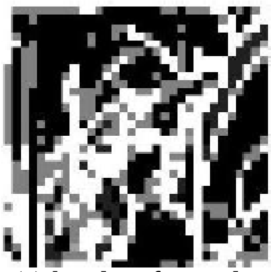

Fig.8. (a)the classify result of HL_4 sub-band coefficient

Fig.8. (b)the classify result of LH_4 sub-band coefficient

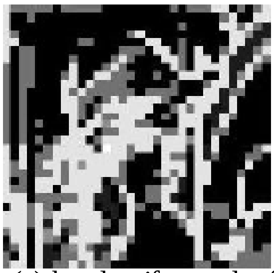

Fig.8. (c)the classify result of HH_4 sub-band coefficient

To verify the robustness of algorithms, we carried out a series of attacks experiment on the image embedded in watermark.

(1)Image JPEG compression:

Fig.9 is the experiment result of image embedded in watermark image with JPEG compressed, JPEG compression quality factor for the values are 10-8.

(a) (b) (c)

Fig.9. the watermark extraction after JPEG compression with different quality factor quality factor=10(b)quality factor=9(c)quality factor=8

The greater the quality factor, the better quality of the watermark recovery, the better the quality of the image. Table 1 lists the similarity (NC) between the watermark taken out and the original watermark and PSNR of watermarked image under different compression ratio. The results prove that the algorithm has good anti-JPEG.

Table1: the experiment result of JPEG compression

Quality factor	Compressi ratio	PNRS	similari (NC)	Retrieved watermark
10	1.4	34.72	0.9995	Fig.7(a)
9	3.6	32.65	0.9340	Fig.7(b)
8	5.4	30.89	0.8253	Fig.7(c)

(2)image noising:

We add Gaussian noise by noise density=1%,5%,10% respectively to Fig.7(a), The extracted watermark image are still recognizable and shown in Fig.10.

We add Salt and Pepper noise by noise density =1%,5%,10% respectively to Fig.7(a), he extracted watermark image are still recognizable(Fig.11).Table 2 shows the experiment result of the image noising.

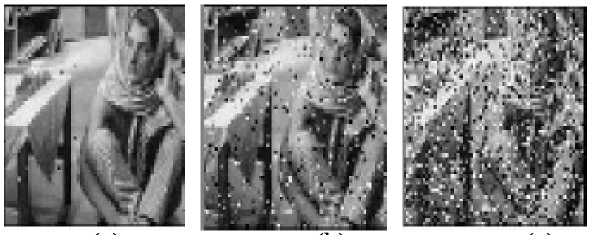

(a) (b) (c)

Fig.10. retrieved watermark after adding different noise.

(a) (b) (c)

Fig.11. retrieved watermark after adding different noise.

Table 2 : The experiment result after adding different noise.

Noise type	Noise density	PNR	similarity (NC)	Retrieved waterma
Gaussian noise	1%	30.81	0.9910	Fig.8(a)
	5%	29.32	0.9184	Fig.8(b)
	10%	27.54	0.7823	Fig.8(c)
Salt & Pepper noise	1%	30.76	0.9765	Fig.9(a)
	5%	28.13	0.9028	Fig.9(b)
	10%	26.83	0.8264	Fig.9(c)

The results prove that the algorithm has strong anti-noise force.

(3)image rotation:

Most watermarking schemes cannot survive after rotation. We rotate Fig.4 32° and resize it to 512×512.The PSNR is seriously reduced to 14.826dB.However,the extracted recognizable watermark image shown in Fig.12 is still extracted.

Fig.12. retrieved watermark after rotation(NC=0.8786)

(4)Image cropping:

Fig.13 shows an inregularly cropped version of Fig.7(a) and Fig.14 shows a cropped version of Fig.7(a) where only the central region, containing the face of Lena remains. Their PSNRs are reduced to 11.3672 and 8.9843, respectively. We can still clearly retrieve the watermark image, as shown in Fig.13(b) and Fig.14(b).

(a) Lena (b) watermark

Fig.13 the watermarked image by irregularly cropping and retrieved watermark

(a) the central of Lena (b)watermark

Fig.14 the central of watermarked image containing the face of Lena and retrieved watermark.

(5)Image filtering:

The detected watermarks are shown in the Fig.15, 3×3 median filtering version of Fig.4.

Fig.15. median filtering experiment result (PSNR=30.23,NC=0.8912)

In this paper, based on characteristics of human visual system, wavelet transform and RBF, an adaptive gray-scale blind watermark algorithm is proposed. The algorithm has the following characteristics:

(1)The compressed 256 gray-scale watermark image after three different scrambling and embedded in different wavelet band. So, enhance the ability of anti-jamming.

(2) Using the characteristics human visual system, adopting the adaptive approach, the vector image wavelet coefficients classified to satisfy different intensity watermark embedded in.So that the algorithm has a good robustness.

(3) Watermark extracted without the original image and the watermark.

The study suggests it is an efficient and robust digital watermarking algorithm using RBF. The embedding scheme results in good quality of the watermarked image. Due to the learning and adaptive capabilities of the RBF, the embedding/extracting strategy can greatly improve the robustness against various attacks. In addition, exhaustive simulation results indicate that the algorithm can apply in the copyright protection and covert communication.

References:

[1]Peter Foris, Dusan LEVICKY, Implementations of HVS Models in Digital Image Watermarking, *Radioengineering*, Vol.16,No.1,2007,pp.45-50.

[2]CAI Su, QI Yue , SHEN Xu2kun, Algorithm for Robust Blind Image Watermark, *Journal of Beijing University of Aeronautics and Astronautics*,Vol 29,No.10, 2003,pp.905-908.

[3]Zhou Ya-xun, Bai Gui-ru, Detection of Image Watermarks with RBF Neural Network in DCT Domain, *Journal of Data Acquisition & Processing*, Vol.16,No.4, 2001,pp.498-503.

[4]Fan Hong, Lei Shi, Ting Luo, A Semi-Fragile Watermarking Scheme Based on Neural Network, Machine Learning and Cyberfnefic, *Proceeding of 2004 Internation Conference on Volume 6*, 2004,pp.3536-3541.

[5]ZHANG Yujin, Image Engneering,*Beijing : Tsinghua University Press* , 2007.

[6]ZHOU Yaxun , BAI Guiru, Detection of Image Watermarks with RBF Neural Network in DCT Domain. *Journal of Data Acquisition & Processing* , 2001 , 16(4) ,pp.4982503.

[7]CHEN B , WORNELL GW, Quantization Index Modulation : A Class of Provably Good Methods for Digital Watermarking and Information Embedding. *IEEE Transactions on Information Theory*, Vol.47, No.4 , 2001, pp.1423-1443.

[8]CHOU C H, LIU K C, Color Image Watermarking Based on A Color Visual Model. *IEEE Workshop on Multimedia Signal Processing*, 2002, pp.367-370.

[9]M. Vairy and Y. V. Venkatesh, Debluring Gaussian Blur Using A Wavelet Arrray Transform, *Pattern Recog*. Vol.28, 1995,pp.965–976.

[10]A. K. Katsaggelos, Digital Image Restoration *Springer-Verlag*, New York, 1991

[11]V. Katkovnik, K. Egiazarian and J. Astola, A Spatially Adaptive Nonparametric Regression Image Deblurring, *IEEE Trans. Image Process.* Vol.14, No.10, 2005, pp.1469–1478.

[12]Y. Yitzhaky and N. S. Kopeika, Identification of Blur Parameters From Motion Blurred Images, Graph.*Model Image Process.*Vol.59,No.5, 1997,pp. 321–332.

[13]P. Guo and L. Xing, Blind Image Restoration Based on RBF Neural Networks, Proc.SPIE 5298, 2004,pp.259–266.

[14]H. Li and P. Guo, The Restoration of Gaussian Blurred Images Using Inverse Principal Element Method, *J. Comm. Comput*, Vol.12,No.1, 2004,pp.64–67.

[15]Y. Xu, J. B. Weaver, D. M. Healy Jr. and J. Lu, Wavelet Transform Domain Filters: A Spatially Selective Noise Filtration Technique, *IEEE Trans. Image Process*,Vol.3,No.6, 1994,pp.747–757.

[16]D. S. Huang, W.-B. Zhao, Determining the Centers of Radial Basis Probabilities Neural Networks by Recursive Orthogonal Least Square Algorithms, *Appl. Math. Comput.*Vol.162, 2005,pp.461–473.

[17]Zhao Dawei, Chen Guanrong, Liu Wenbo, Achaos-Based Robust Wavelet-Domain Watermarking Algorithm. *Chaos, Solitons and Fractals*,Vol. 22,2004,pp. 47-54.